

Title	ECR Plasma in a High Power Millimeter-Wave Beam (Report 1)(Welding Physics, Process & Instrument)
Author(s)	Arata, Yoshiaki; Miyake, Shoji; Abe, Nobuyuki et al.
Citation	Transactions of JWRI. 1984, 13(2), p. 181-185
Version Type	VoR
URL	<a href="https://doi.org/10.18910/10987">https://doi.org/10.18910/10987</a>
rights	
Note	

*Osaka University Knowledge Archive : OUKA*

<https://ir.library.osaka-u.ac.jp/>

Osaka University

# ECR Plasma in a High Power Millimeter-Wave Beam (Report 1)<sup>†</sup>

Yoshiaki ARATA\*, Shoji MIYAKE\*\*, Nobuyuki ABE\*\*\*, Hiroaki KISHIMOTO\*\*\*\*,  
Yoshiaki AGAWA\*\*\*\*\* and Yoshinobu KAWAI\*\*\*\*\*

## Abstract

*Using a high power millimeter-wave beam of Gyrotron, ECR plasma production and heating are experimentally studied. Characteristic features of 60 GHz Gyrotron used in the experiment are described with the program plan on the efficient usage of this millimeter-wave beam to high temperature plasma production and surface heating of materials. Preliminary experimental results in Ar gas are reported indicating a high density plasma production with  $n_e \simeq 10^{13} \text{ cm}^{-3}$  and with a strong X-ray radiation at a pressure over  $1 \times 10^{-1} \text{ Pa}$ .*

**KEY WORDS:** (ECR Plasma) (Millimeter-Wave) (Gyrotron) (Soft X-ray) (Multiply-Charged Ion)

## 1. Introduction

In the conventional microwave tubes of magnetron, klystron and/or TWT, oscillation mechanism is based on the non-relativistic motion of electrons in a cavity. In these tubes output power and its efficiency are lowered drastically as the scale of the circuit structure becomes too small in the millimeter wavelength regions. While in recent nuclear fusion research, high power tubes of "Gyrotron" are extensively used<sup>1)</sup> for the electron cyclotron heating of plasmas. Oscillation mechanism<sup>2)</sup> in Gyrotron is the coherent emission of radiation by electrons having a weakly relativistic cyclotron motion in a strong magnetic field. Basically they can obtain unusually large power levels at short wavelengths as the frequency is fixed only by the strength of an externally applied magnetic field, rather than by the scale of cavities. This fact also motivates the application of a steady or a quasi-steady high current hollow beam of high energy electrons, since only transverse energy of the beam is converted into electromagnetic radiation. By these properties Gyrotron is sometimes called Electron Cyclotron Maser (ECM)<sup>3)</sup>.

In 1983 we installed a 60 GHz high power Gyrotron at the Research Center for Ultra-High Energy Density Heat Source. It can generate the maximum radiation power of 200 kW in a quasi-steady state up to 100 ms at a wavelength of 5 mm and an energy density over  $10^5 \text{ W/cm}^2$  is

expected by the strong focusing with a quasi-optical waveguide system. At installation we have settled following four research themes as the program plan by the gyrotron of a new type high energy density heat source: i) study on ECR (electron cyclotron resonance) high temperature plasma, ii) research and development on plasma soft X-ray source, iii) research and development on ECR ion source including production of multiply-charged ion beam, iv) study on surface heating of materials.

Items i) ~ iii) are closely connected each other and the first of them is the key problem for the second and the third. At present we are devoting to the first and the fourth will start in near future.

Researches on ECR plasma are widely distributed such as in nuclear fusion<sup>4)</sup>, electrical discharge problem<sup>5)</sup> and in the application to ion source<sup>6)</sup> or plasma CVD<sup>7)</sup>. In our study plasmas in various gas species are produced in a simple mirror magnetic field. Incident microwave energy to the mirror field is dissipated in the ionization of neutral gas and efficient heating of the plasma to a high temperature state. Experiments so far in a simple mirror field have been performed in the microwave frequency below or around 10 GHz and the gas pressure ranged between  $10^{-4}$  to  $10^{-2} \text{ Pa}$ . The power input in the quasi-steady state is lower than 10 kW. As the ionization of neutral gas by the wave develops rapidly due to the coherent acceleration of

<sup>†</sup> Received on October 31, 1984

\* Professor

\*\* Associate Professor

\*\*\* Research Instructor

\*\*\*\* Graduate Student

\*\*\*\*\* Professor, Kyushu University

electrons at the cyclotron resonance condition, an almost fully ionized plasma is obtained rather easily. But the wave angular frequency  $\omega$  limits the electron density  $n_e$  by the relation  $\omega (= \omega_{ce}) \geq \omega_{pe}$ . Here  $\omega_{ce}$  is the electron cyclotron frequency and  $\omega_{pe}$  is the plasma frequency which is defined to be  $\sqrt{n_e e^2 / m_e \epsilon_0}$ , where  $e$ ,  $m$  and  $\epsilon_0$  are electron charge, electron rest mass and permittivity of free space, respectively. The limiting value of  $n_e$  is attainable by increasing the gas pressure  $p_0$  and sometimes plasma density over the critical one is reported<sup>8)</sup>. In this case, however, the electron temperature  $T_e$  is very low and typically lower than 10 eV and any X-ray emission is not observed. Dominant collision process cancels out the heating of electrons to a higher temperature.

Applying our gyrotron we aim at obtaining a high density and/or a high temperature plasma of  $n_e = 10^{12} \sim 10^{13} \text{ cm}^{-3}$ ,  $T_e = 0.1 \sim 1 \text{ keV}$ . These values are important and very comfortable for the study of the second and the third themes. As for  $n_e$  it seems to be not difficult to obtain, since the limiting value of  $n_e$  by the wave frequency  $\omega$  reaches to  $4.5 \times 10^{13} \text{ cm}^{-3}$ . Only we need is to increase the gas pressure up to  $2 \times 10^{-1} \text{ Pa}$ , where the neutral particle density  $n_0$  is  $4.8 \times 10^{13} \text{ cm}^{-3}$  at room temperature. We further remark the fact that in our experiment the power input is larger in a quasi-steady state by one order than in any other experiments previously reported. We expect that very strong pumping would cause not only a fully ionized plasma but also extensive heating to a high temperature over 0.1 keV at  $p_0 \sim 10^{-1} \text{ Pa}$ .

This paper describes preliminary experimental results as the first of the series of reports according to the addressed program plan.

## 2. Experimental Apparatus

Figure 1 shows a bird's-eye view of the apparatus installation. The Gyrotron and its power supply system are settled on the floor. A vacuum chamber and superconducting (SC) mirror coils are located in the basement to produce a high temperature plasma. A millimeter wave beam from the Gyrotron is transmitted through cylindrical waveguides of 2.54 cm in diameter to the vacuum chamber. The basement is separated by a concrete wall of 50 cm thick and a lead door from the adjoining room used for the arrangement of the diagnostic system. While observation is performed in a room screened by the concrete wall on the same floor with the Gyrotron.

Figure 2 shows schematic diagram of the Gyrotron (VGE 8060, Varian). It has a specification of 60 GHz in  $TE_{02}$  mode and the maximum output power of 200 kW

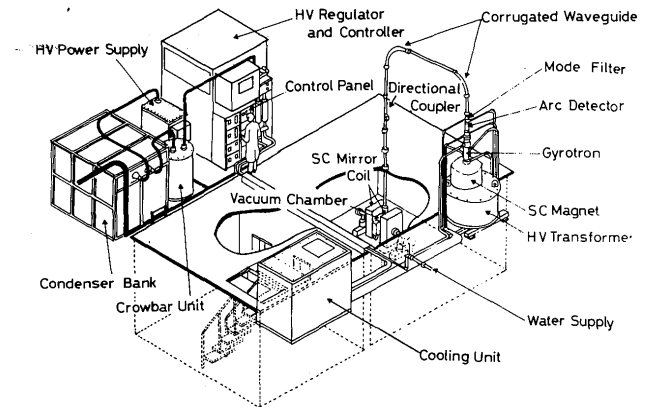


Fig. 1 Bird-eye's-view of experimental apparatus

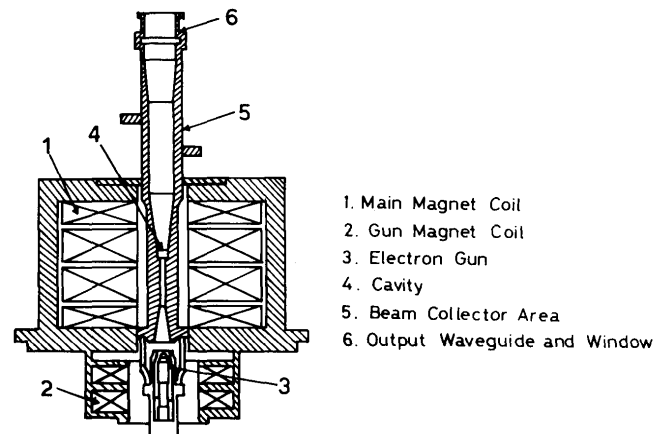


Fig. 2 Schematic diagram of gyrotron and SC coil system

with the maximum pulse length of 100 ms. Within the Gyrotron tube a hollow beam of electrons from a magnetron injection type electron gun enters into the cavity in a strong field supplied by the main magnet coil. It radiates coherent millimeter wave radiation with a high efficiency of 30 ~ 40% and is collected in the beam collector area. The wave propagates through an BeO output vacuum window into the arc detector that is shown in Fig. 1. The arc detector protects the Gyrotron against arcing within the waveguide by detecting an emission signal from the arc and cutting off the high voltage to the tube. Over 90% of the output power is specified to be in the  $TE_{02}$  mode. To reduce the other mode a mode filter is inserted after the arc detector. At the exit of the filter a tapered waveguide is mounted to reduce the diameter of the oversized waveguide from 6.25 to 2.54 cm and is connected to the corrugated waveguide without remarkable power loss. The waveguide diameter is widened again to 6.25 cm, when the wave beam enters into chamber sealed by an BeO window.

During the operation of the Gyrotron, electron beam voltage  $V_B$ , beam current  $I_B$  to the collector area and the

body current  $I_b$  to the anode of the gun are always monitored on an CRT. Special attention is paid to the change of  $I_b$ , as the gun is apt to be damaged at its high value because of the arcing within the tube. It is always kept below 20 mA.

The main magnet coil current is controlled by two power supplies. One is used for the current control of the upper two segments of the coil and the other for the lower two. Here the former current is labeled as  $I_1$  and the latter as  $I_2$  and the current in the gun magnet coil is labeled as  $I_3$ . Good operating conditions of the Gyrotron is found by appropriate selection of these values.

In order to match the wave frequency of 60 GHz to electron cyclotron resonance and to confine the plasma, a strong mirror magnetic field is prepared by two superconducting coils around the vacuum chamber. The coils are made of Nb-Ti and the boil-off of the liquid helium at operation is 2  $\ell$ /h per coil. The vacuum chamber is made of aluminum whose overall length in the axial direction is 74 cm and the radial dimension has 43.6 cm at the center. Schematic of the chamber configuration is drawn in Fig. 3 with the magnetic line of force. Mirror ratio (MR) can be varied by changing the distance between two mirrors from 2.0 to 4.6. Figure 3 shows the distribution of magnetic flux density and magnetic line of force in case of MR = 2. Distance between mirrors is 37.5 cm. At the maximum coil current of 300 A, the flux density  $B$  is 2.7T at the throat of the mirror. The flux density corresponding to the 60 GHz fundamental resonance frequency is 2.0T as shown in the figure. The second harmonics is also shown

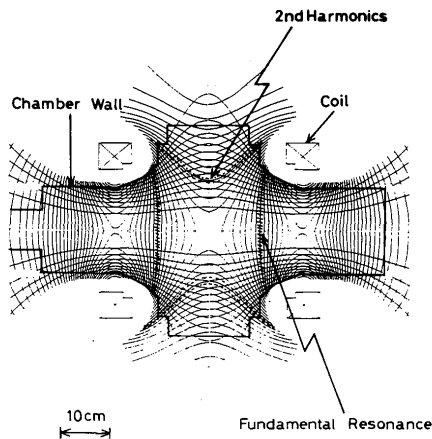


Fig. 3 Magnetic line of force and flux density at MR = 2

by the broken line. A 500  $\ell$ -turbomolecular pump evacuates the chamber to a base pressure of  $10^{-5}$  Pa and various gas species are used for experiments in the range of  $p_0 = 10^{-3} \sim 10^0$  Pa.

Figure 4 shows schematic diagram of diagnostic system of the ECR plasma. The hot electron temperature  $T_e$  is decided by the pulse height analysis of X-rays from the plasma. The X-ray detection is carried out by the pure Ge

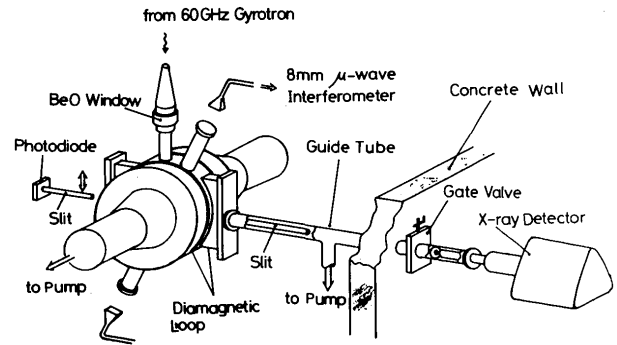


Fig. 4 Schematic of diagnostic system of the plasma.

or Si(Li) semiconductor detector. To reduce the loss of soft X-ray within the guide tube, the tube is evacuated and the lead collimator is inserted to detect the X-ray only from the plasma itself.

The electron density  $n_e$  is decided by using an 8 mm-microwave interferometer. Measurement is performed perpendicular to the magnetic axis and the maximum density to be detectable is  $1.75 \times 10^{13} \text{ cm}^{-3}$ . Two loops each of which has 25-turns are wound around the chamber near at the center for evaluating the diamagnetism of the plasma. By the time integration of the loop voltage, stored energy by the hot electrons is estimated. A radial distribution of visible light from the plasma is measured with a photodiode. It is moved along the chord of the plasma and the distribution can be obtained as a function of time. Also by replacing the X-ray detector with a VUV spectrometer various line spectra can be measured to estimate the multiplicity in the ionization stage.

### 3. Preliminary Result and Discussion

Figure 5 shows a typical example of  $V_B$ ,  $I_B$ ,  $I_b$  for a pulse length  $\tau_\mu = 40$  ms. RF output detected by the direc-

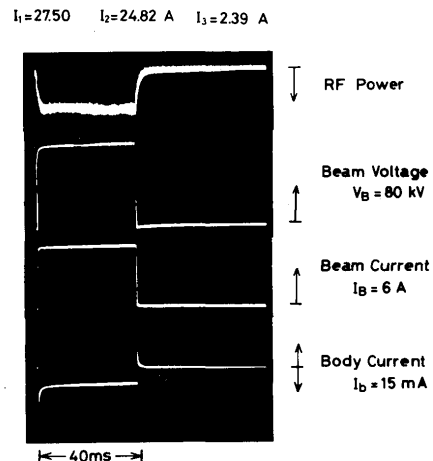


Fig. 5 Typical gyrotron operation parameters for  $\tau_\mu = 40$  ms

tional coupler is also shown. In this case the wave is absorbed by a water load mounted after the directional coupler and all pulse shape show a stable operation of the tube. In Fig. 6 is shown the output power  $P_i$  versus  $I_1$  at a fixed value of  $I_2$  and  $I_3$ . The power is decided by the temperature rise of the water load. In this report the pulse length of the wave is fixed to 40 ms for all experimental runs.

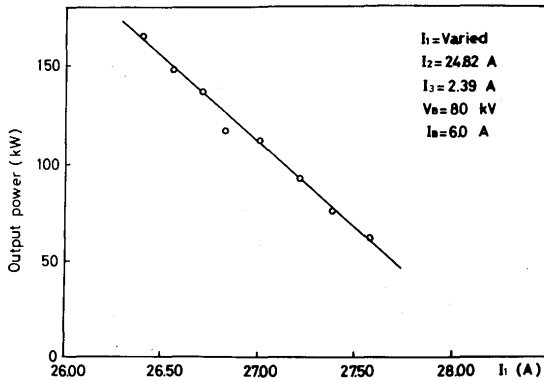


Fig. 6 Output power of the gyrotron versus current of the main magnetic coil

Figure 7 gives a typical example of various detector signals from the ECR plasma in Ar gas. As stated in the introduction we have performed experiments at a gas pressure over  $1 \times 10^{-1}$  Pa. A stable plasma production and heating is clearly found from these data. For instance visible emission detected by the photodiode shows a peak in the early stage of the pulse duration and decreases sharply due to the efficient heating process. It reaches to a quasi-steady state at about  $t = 20$  ms. We must note here that this data might also reflect the decrease in the plasma density due to the lowering of the gas pressure by the transient plasma production and heating processes. In (d) of the figure a variation in  $n_e$  during the power input is clearly seen and a rapid cut-off of the interferometer input by the plasma is found at the starting point of the plasma production. As stated earlier the cut-off density of the interferometer is  $1.75 \times 10^{13} \text{ cm}^{-3}$  and we have successfully obtained a high density plasma of  $n_e \approx 10^{13} \text{ cm}^{-3}$ . By using a nude gauge, time variation of  $p_0$  will be measured and be correlated with that of  $n_e$  and the result will be described in the next report.

Development of the plasma diamagnetism well corresponds to the hot electron production as shown in (c) and (e) of the figure. After about 20 ms from the RF power input, the diamagnetic signal develops with time and begins to decay slowly after the wave off. It indicates that trapped hot electrons are losing their energy by ionizing collisions with the back ground neutral gas at the time without energy input. So that a slight visible light emission and strong X-ray radiation lasts until about

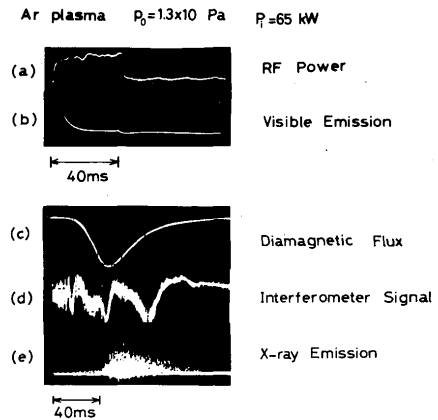


Fig. 7 Typical example of various detector signals from the plasma in Ar gas

$t = 100$  ms. Slow decrease of electron density is also verified in (d) at  $t > 40$  ms.

As for the time variation of the RF power in the figure, it differs remarkably from the one in Fig. 5. It will, of course, be caused by the variation of the plasma as a load but at present the problem is not answered so clearly, since at a high power input the characteristic of the directional coupler is apt to deviate from a small signal one and the change in the plasma load may possibly modify the properties of the Gyrotron operation.

We have measured VUV emission with a Seya-Namioka Type spectrometer ( $F = 50$  cm, Nikon). Figure 8 shows time variation of several Ar lines. During the plasma production and heating the neutral line decays at a very short time and the higher the charge state the later the time when the peak of the line emission appears. It indicates that the heating of the plasma is remarkably progressing with time.

The X-ray radiation detected by the pure-Ge semiconductor is processed through a CAMAC-PHA system and is displayed as an X-ray spectrum. As shown in

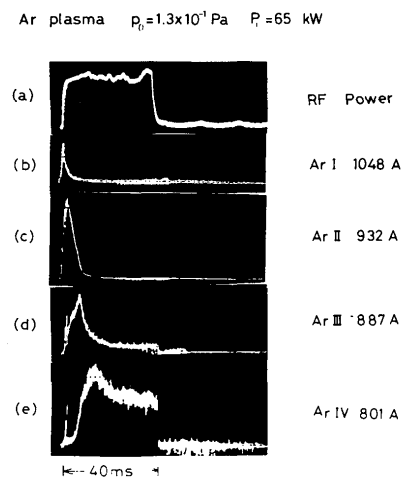


Fig. 8 Time variation of several VUV line spectra

Fig. 8-(e), X-ray radiation begins to increase from about 10 ms after the power input and continues until 100 ms in conjunction with the variation of the diamagnetic signal. **Figure 9** shows an example of a raw data of the time integrated X-ray spectrum with summation over 10 shots of the discharge. It is clear that a strong soft X-ray continuum is obtained with a superposition of  $K_{\alpha}$ -line of Ar around 3 keV. It also has a tail in the high energy region. With several calibration and cross-checking procedures, the electron temperature will be decided for various parameters. We will also report on the time variation of  $T_e$  in the next paper.

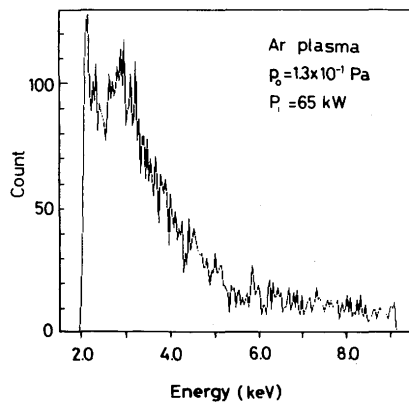


Fig. 9 An example of the time integrated plasma X-ray spectrum

#### Acknowledgement

The authors would like to express their gratitude to Prof. M. Ushio, S. Kawanishi and T. Yamamoto for their interest and critical comments to this study. They also thank to Dr. K. Sato for his support in the detection of VUV spectra.

#### References

- 1) A.V. Gaponov et al.: *Izv. Vuz. Radiofiz.* **18** (1975), 280.
- 2) A.V. Gaponov: *Izv. Vuz. Radiofiz.* **2** (1959), 450.
- 3) J. Schneider: *Phys. Rev. Lett.* **2** (1959), 504.
- 4) D.E. Baldwin and TMX-U Group: *Plasma Physics and Controlled Fusion* **26** (1984), 227.
- 5) Y. Kawai and K. Sakamoto: *Rev. Sci. Instrum.* **53** (1982), 606.
- 6) J. Ishikawa et al.: *Rev. Sci. Instrum.* **55** (1984), 449.
- 7) T. Ono, Y. Adachi and S. Matsuo: *Proc. Int. Ion Engineering Congress*, 1983, p. 753.
- 8) Y. Sakamoto et al.: *Jpn. J. Appl. Phys.* **16** (1977), 1983.